COMMISSARIAT A L'ENERGIE ATOMIQUE

CENTRE D'ETUDES NUCLEAIRES DE SACLAY
Service de Documentation
F91191 GIF SUR YVETTE CEDEX

CEA-CONF -- 7946

L3

Rapport DPh-N/Saclay n°2275 06/1985

SOME ASPECTS OF HEAVY ION PHYSICS BETWEEN 20 AND 50 MeV/U

Christian Ngô

Service de Physique Nucléaire - Métrologie Fondamentale
CEN Saclay, 91191 Gif-sur-Yvette Cedex, France

Communication présentée à : Course on nucleus-nucleus collisions from the coulomb barrier up to the quark-gluon plasma
Erice (Italy)
10-22 Apr 1985

SOME ASPECTS OF HEAVY ION PHYSICS BETWEEN 20 AND 50 MeV/u

Christian NGÔ
Service de Physique Nucléaire - Métrologie Fondamentale
CEN SACLAY, 91191 Gif-sur-Yvette Cedex, France

Heavy ions like Ar or Kr are now available at bombarding energies between ~ 20 and 50 MeV/u at GANIL or SARA. They can be used to investigate what happens when a heavy projectile interacts by nuclear forces with a heavy target. This will permit to understand how the mechanisms evolve from the low energy domain, dominated by the mean field, to the high energy region, dominated by the nucleon-nucleon interaction. Many experiments have now been performed in this intermediate energy domain and a lot of experimental data have been obtained. In these lectures we shall try to present some aspects of these results and see whether some general features emerge in this bombarding energy region.

1 - In the first lecture we shall sumarize the results which have been obtained in the experiments where one looks at how much linear momentum the projectile can transfer to a fused system. In this energy domain the fusion process, when it is still present, is incomplete in the sense that several light particles can be emitted before the fusion process takes place. We shall also estimate the maximum amount of energy that one can deposit in a nucleus and see that this might be one limitation for preventing the fusion of two nuclei during a long time.

2 - In the second lecture we shall describe very recent results obtained with Kr projectiles. We shall see that, at variance with Ar ions, one observes a large proportion of events with a mass and a kinetic energy substantially smaller than the one of the projectile. These products could possibly be understood as resulting from a mechanism similar to calefaction, a phenomenon familiar in our macroscopic world.

3 - Finally, in the last part we shall investigate, from the theoretical point of view, whether nuclei could be mechanically unstable. This will be done in the framework of a time dependent Thomas Fermi approach. We shall see that compression, can be a cause of mechanical instability.

ACKNOWLEDGMENT

I am very grateful to Mrs F. Lepage and E. Thureau for their careful preparation of the manuscript.

LINEAR MOMENTUM TRANSFER

C. Ngô and S. Leray

Service de Physique Nucléaire - Mesures Fondamentales
CEN Saclay, 91191 Gif-sur-Yvette Cedex, France

INTRODUCTION

One of the goals of heavy ion collisions has always been to perform the fusion of two nuclei and to study the properties of the formed system (Ngô, 1985). This was always possible at low bombarding energies (E/A < 10 MeV/u, where E/A denotes the bombarding energy per nucleon) provided that the product, $Z_1 Z_2$, of the atomic numbers of the projectile and of the target is not too large ($Z_1 Z_2$ < 2500-3000), and that the bombarding energy is large enough to surmount the coulomb barrier between the two nuclei. However, with heavy projectiles, like Kr or heavier ones, and heavy targets, like Au for instance (Lefort, 1973), fusion is no longer possible due to the coulomb force between the two nuclei which becomes too strong to be counteracted by the nuclear force. In this bombarding energy region the fusion of two nuclei is complete in the sense that all the nucleons of the projectile and of the target merge in a single system which, in many cases can be identified with a compound nucleus. In other situations one only forms a two center equilibrated system which subsequently fissions (fast fission (Ngô, 1985)). As the bombarding energy is raised above 8-10 MeV/u the fusion of the nuclei is no longer complete because prompt particles (neutrons, protons, alphas) are emitted before the two remaining parts of the projectile and of the target fuse. In this case one is used to call the fusion of a part of the projectile with a part of the target : incomplete fusion (Siemssen, 1983). Several explanations have been proposed for the emission of these prompt particles : promptly emitted particles or Fermi jets (Bondorf, 1980; Robel 1979; Davies 1984; Leray 1985), pre-equilibrium emission (Griffin, 1966; Blann 1968), decay of a hot spot (Sobel, 1975; Weiner, 1977) inertial emission (Grégoire, 1983; Tricoire, 1984). These particles are very fast in the laboratory system if they are emitted by the projectile otherwise, if they are emitted by the target, they are very slow. An important point is that the number of prompt particles increases when the bombarding energy increases over ~ 8-10 MeV/u. The investigation of incomplete fusion is a big puzzle and the measurement of the amount of linear momentum (LM) transferred from the projectile to the fused system is one of the pieces of this puzzle. New accelerator facilities can accelerate heavy ions at bombarding energies up to ~ 50-100 MeV/u and several studies have been devoted to the study of the amount of LM transferred from the projectile to the fused system in the energy range going from 20 to almost 100 MeV/u (Sikkeland, 1968) (Viola, 1982). The aim of this lecture is to give a brief overview of the present experimental situation in this domain as well as of the remaining open problems.

I. EXPERIMENTAL METHOD

In incomplete fusion reactions one forms an excited system which will de-excite either by emitting light particles and γ-rays, or by fissioning. By measuring some of the properties of the nuclei created after the de-excitation one gets informations about, p, the amount of LM transferred from the projectile to the fused system. Two experimental methods have been used so far : one based on the fission fragment angular correlation technique and the other one on the evaporation residues velocity spectrum. However, they cannot be always applied simultaneously because evaporation residues and the fission fragments do not necessarily occur with a measurable probability for a given system. Indeed, heavy nuclei mainly de-excite by fission whereas light ones lead essentially to evaporation residues. Only medium nuclei can be investigated by both methods.

a) The fission fragments correlation techniques

In complete fusion the recoiling nucleus has a velocity, V_R, which is equal to the velocity of the center of mass of the total system, V. Therefore, in the laboratory system, the fold-

ing angle, ϑ_f, between two fission fragments of given kinetic energy can be easily calculated and is constant. For incomplete fusion $V_R < V$ because prompt particles have been emitted prior to fusion. Therefore, they remove a part of the initial LM. It follows that, for the same fission products as those discussed above, ϑ_f, will be larger. In the extreme case where the amount of LM transferred is zero, $\theta_f = 180°$. The measurement of ϑ_f then allows to deduce the amount of LM transferred from the projectile to the fused system. This technique has been successfully introduced a long time ago (Sikkeland, 1968) at low bombarding energy where full momentum transfer was always achieved.

Actually, the experimental measurement is not as simple as described above because one does not detect the primary fission fragments but only the secondary products after de-excitation of the primary ones. Furthermore, in a fission process one gets fragments with a distribution in kinetic energy, mass and atomic number. One usually proceeds as follows : one puts a detector at an angle θ_3 with respect to the beam axis in order to detect one of the fission fragments. These two directions define a plane which is usually the horizontal plane of the experimental set-up. The second fragment is detected on the other side with respect to the beam axis but not necessarily in the horizontal plane. Let us call ϕ_4 the angle between the direction of the second fragment and the horizontal plane (out of plane angle) and θ_4 the angle between the perpendicular projection of this direction on to the horizontal plane and the beam axis (in plane angle). The measured quantity is the probability distribution $W(\theta_3, \theta_4, \phi_4)$ which gives the probability of detecting a second fragment at θ_4, ϕ_4 when one detects the first one at θ_3. It is convenient to introduce two reduced probability distributions $p(\theta_3, \theta_4)$ and $q(\theta_3, \phi_4)$ which are obtained by integration of W with respect to ϕ_4 or θ_4 using the proper jacobian ($\cos\phi_4$). The probability distributions are not delta functions because of several effects :

i) The fission fragments are excited, therefore they will de-excite by light particle evaporation. This will induce a broadening of the distributions around a mean value. This broadening is the same in and out of the reaction plane.

ii) The fission fragments have a mass and a kinetic energy distribution which will induce a broadening of the $p(\theta_3, \theta_4)$ correlation.

iii) For incomplete fusion the recoil velocity of the fissioning nucleus will have a distribution around a mean value. This will also lead to a broadening in an out of the reaction plane.

In order to illustrate the kind of probability distribution that one obtains in such experiments we present, in Fig. 1 and 2, $p(\theta_3, \theta_4)$ and $q(\theta_3, \phi_4)$ for the Ne + Au system at 30 MeV/u investigated in ref.(La Rana, 1983). In Fig. 1 the arrow indicates the angle θ_4 corresponding to full linear momentum transfer. The experimental points which are on the left of this arrow are due to points i) and ii) above. They of course do not correspond to a LM transfer greater than 100 %. The first result which can be extracted from Fig. 1 is the most probable folding angle $\theta_3 + \theta_4$ which corresponds to 77 % of the initial linear momentum transferred to the fused system. It is difficult to get more information from Fig. 1 because it is not easy to make a deconvolution of the three physical effects described above (i, ii, iii). A better way to proceed is to perform a simulation as it was done in ref. (La Rana, 1983). The result of this Monte-Carlo simulation corresponds to the full line in Fig. 1. It agrees well with the data except for large θ_4 values. This is due to the fact that this calculation does not take into account of the sequential fission of the Au target after it has experienced a grazing collision. This sequential fission mechanism gives three bodies in the exit channel. The two fission fragments resulting from this interaction give a correlation function centered around $\theta_f \sim 170\text{-}180°$. The simulation reproduces also quite well the out of plane distribution (Fig. 2) which is essentially due to evaporation. The standard deviation of the calculated $p(\theta_3, \theta_4)$ distribution is equal to $\sigma_{\theta_4} = 8.96°$ and to 5.93° for $q(\theta_3, \phi_4)$. It is interesting to give here the standard deviations corresponding to each of the physical effects (taken alone) which contribute to a broadening of the in plane and out of plane distributions. Table I gives the results of these calculations assuming that there is no perpendicular distribution of ρ perpendicular to the reaction plane. Table I shows that one has to be very careful in analysing the experimentalo datas. It is also worth to note that many experiments perform measurements only in the horizontal plane. Therefore, one gets $W(\theta_3, \theta_4, 0)$, a quantity which is supposed to be proportional to $p(\theta_3, \theta_4)$. This statement is only true if the shape of out of plane distribution does not change as a function of θ_4. This is approximatively valid for the Ne + Au system but might not be so for other projectile-target combinations.

a) The evaporation residues velocity spectrum

When evaporation residues are formed with a non-negligeable probability, a simple way to get informations about the amount of LM transferred from the projectile tc the fused system is to measure their velocity spectrum (Cerruti, 1983). The most probable velocity allows to calculate $\vec{\rho}$ since $\vec{V}_R$ it is not changed by evaporation. A simulation can also permit tc estimate the distribution of ρ around $\vec{\rho}$. The most interesting systems to investigate by this method are

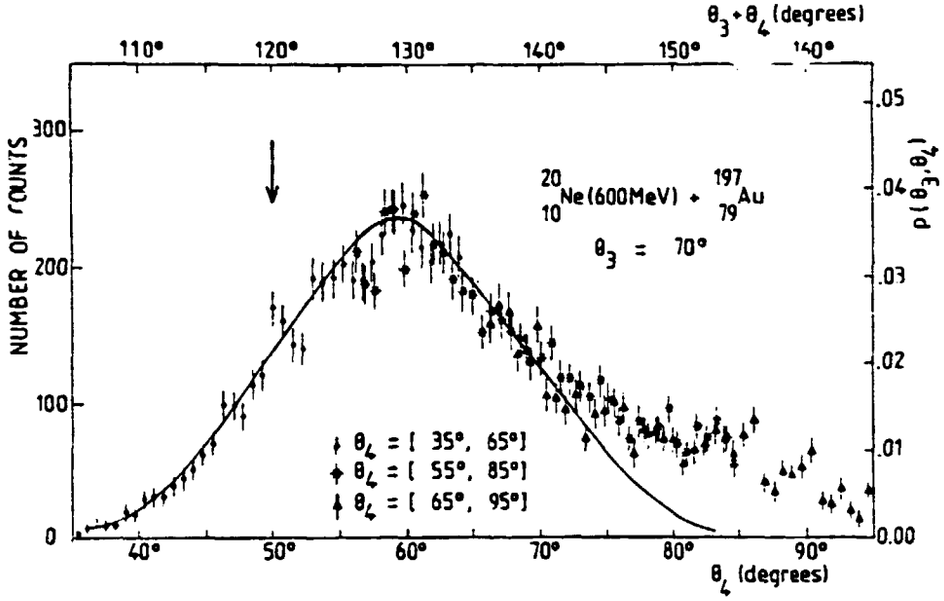

Fig. 1. Correlation function $p(\theta_3, \theta_4)$ versus θ_4 representing the in plane angle distribu-tribution. The arrow indicates the folding angle associated with full momentum transfer. The full line is a result of a Monte-Carlo simulation. From ref.(La Rana, 1983).

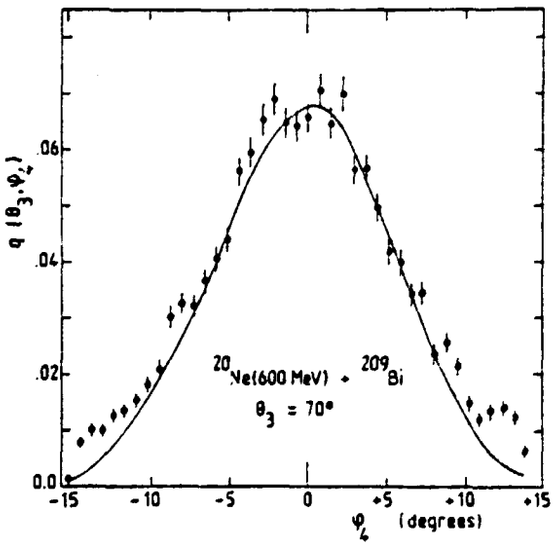

Fig. 2. Correlation function $q(\theta_3, \phi_4)$ versus ϕ_4. The full line is a result is a result of a Monte-Carlo simulation. From ref.(La Rana, 1983).

those which give a fused nucleus which de-excite either by fission or by particle evaporation because one can get $\tilde{\sigma}$ by two different experimental methods. This is interesting because it is not the same orbital angular momentum values which are involved and this might provide a way to investigate the dependence of $\tilde{\rho}$ on angular momentum. The Ar + Ag is a good candidate for such studies. At 19.6 MeV/u one gets the same value of $\tilde{\rho}$ by the two methods (C. Cerruti, 1985) whereas at 27 MeV/u it was found that they differ (Borderie, 1985).

Table I Results of the Monte-Carlo simulation used to investigate the influence of different effects on the in-plane (θ_4) and out-of-plane (ϕ_4) distributions for the Ne + Au system (σ_{θ_4} and σ_{ϕ_4} are the standard deviations of the distributions with the mean values $\langle\theta_4\rangle = 60°$ and $\langle\phi_4\rangle = 0°$). From ref.(La Rana, 1983).

Effect	σ_{θ_4} (degrees)	σ_{ϕ_4} (degrees)
size of the solid-state detector	0.38	0.38
mass distribution	1	0
kinetic-energy distribution	2	0
particle evaporation	5.93	5.93
parallel linear-momentum distribution	6.35	0
full simulation	8.96	5.93

II. SUMMARY OF THE EXPERIMENTAL RESULTS

Most of the experimental investigations concerning LM transfer have been made with light projectiles (< Ne) using the fission fragment angular correlation technique. In all the cases the folding angle distribution is similar to the one displayed in Fig. 1. It was found that, $\tilde{\rho}$, the most probable amount of LM transfer decreases as the bombarding energy per nucleon increases. The quantity ρ is defined quantitatively as the ratio between the initial LM and the LM associated with the fused system. According to this definition $\rho=1$ for full momentum transfer and $\rho=0$ for no momentum transfer. As it has been proposed in ref.(Viola, 1982) one can plot $\tilde{\rho}$, the most probable value of ρ, as a function of E/A for some of the systems investigated with light projectiles. This is displayed in Fig. 3. One first sees that all the systems seem to have a similar evolution. Below E/A < 3.2 $(MeV/u)^{1/2}$ there is full momentum transfer whereas $\tilde{\rho}$ decreases almost linearly above this value. The mean evolution of the experimental points can be parametrized as follows (La Rana, 1983) :

$$\tilde{\rho} = -\,0.0092\sqrt{\frac{E}{A}} + 1.273 \qquad \text{for} \qquad \sqrt{\frac{E}{A}} > 3.2\ [MeV/u]^{1/2}$$
$$\tilde{\rho} = 1 \qquad \text{for} \qquad \sqrt{\frac{E}{A}} < 3.2\ [MeV/u]^{1/2} \qquad (1)$$

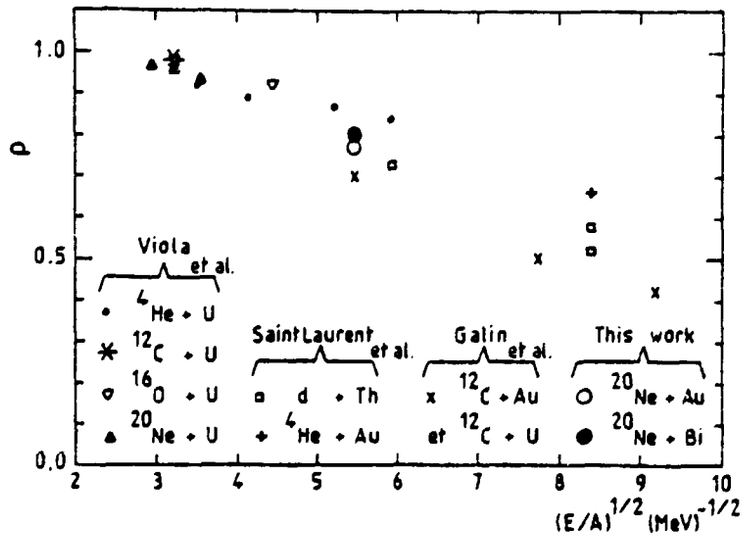

Fig. 3. Most probable amount of LMT from the projectile to the fused system plotted as a function of the square root of the incident energy per nucleon for different systems. From ref.(La Rana, 1983).

It is interesting to see how general the above systematics work when one uses heavier projectiles. Several experiments have been now performed (Charvet, 1984; Borderie, 1984) with Ar beams at GANIL and SARA. It was found that for bombarding energies equal to 19.6 and 27 MeV/u, $\tilde{\rho}$ still behaves as indicated in eq.(1) but at yet higher energies this is no longer the case. This is illustrated in Fig. 4 where one shows the in plane angle correlation function for the Ar + U system at 3 different bombarding energies : 19.6 MeV/u (Leray, 1985), 27 MeV/u (Jacquet, 1985), 35 MeV/u (Leray, 1985) and 44 MeV/u (Leray, 1984; Charvet, 1984). As we can see, the 19.6 MeV/u results of Fig. 4 show two pronounced peaks. The first one, located at about $\theta_f = 120°$ corresponds to fission following incomplete fusion. From the most probable value of θ_f one can deduce $\tilde{\rho} = 0.86$. The second peak, located roughly at $\theta_f = 170°$, can be ascribed to inelastic scattering of the incident Ar projectile, followed by the sequential fission of the excited U nucleus. A similar situation is observed at 27 MeV/u (Jacquet, 1985). However at 35 and 44 MeV/u the correlation functions are quite different. The first peak at low θ_f has disappeared while the peak associated with sequential fission is still present. It is not possible to extract a $\tilde{\rho}$ value for incomplete fusion. However, since sequential fission cannot readily contribute to the counts in the region where θ_f is lower than 140°, it seems as there remains a certain contribution of incomplete fusion events. Nevertheless, the most probable value $\tilde{\rho}$ of ρ is certainly different from the one predicted by eq.(1).

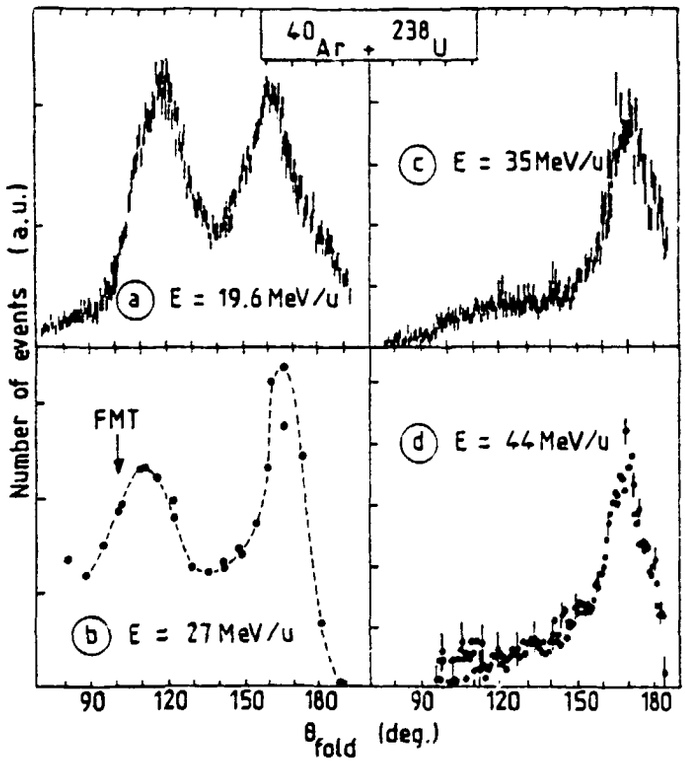

Fig. 4. Folding angle distribution of the fission fragments associated with the Ar + U system at different bombarding energies : 19.6 MeV (Leray, 1985) ; 27 MeV/u (Jacquet, 1985); 35 MeV/u (Leray, 1985) and 44 MeV/u (Charvet, 1983).

The conclusion of these studies is that $\tilde{\rho}$ does not only depend on E/A but that it seems also to depend on the size of the projectile. If the systematics of eq.(1) would be valid for any combination of projectiles and targets it would mean in particular that $\tilde{\rho}_1$ oberved in a A_1+A_2 reaction is identical to $\tilde{\rho}_2$ measured in the inverse kinetics A_2+A_1. The experimental knowledge of $\tilde{\rho}$ in the above reactions would be more than welcome because it will then settle the question of the number of particles emitted before fusion by the projectile and the target respectively. Indeed, $\tilde{\rho}$ is a laboratory quantity and not a property of the center of mass system. It is mostly sensitive to the number of prompt particles emitted by the projectile prior to fusion. This means that there is a priori no reason why $\tilde{\rho}$ should be the same for the normal (A_1+A_2) and for the inverse kinematical reaction (A_2+A_1). A simple model, presented in (Ngo, 1985) indeed shows that $\tilde{\rho}_1$ and $\tilde{\rho}_2$ should be different.

3. MAXIMUM ENERGY CONTENT OF A NUCLEAR SYSTEM

In incomplete fusion there is a global statistical equilibrium of the fused system. This means that one has a constant temperature over the whole volume. Therefore, it is reasonable to think that it will not be possible to provide too much excitation energy to the fuse nucleus otherwise there will be a total ebullition and it will not be possible to observe fission fragments, nor evaporation residues. The question of how much energy one can deposit in a nucleus turns out to be of crucial importance and we shall describe here the simple answer to this problem given in (Leray, 1985).
If the ebullition of a nucleus would give a gas of free nucleons, one has to consider the following reaction mechanism :

$$\text{Nucleus} \overset{(1)}{\rightleftarrows} \text{neutrons} + \text{protons} \qquad (2)$$

The energy necessary to do that is equal to $A\,\varepsilon_B$, where A and ε_B are the mass and the binding energy per nucleon respectively. Using the usual A value for the level density parameter, which relates the excitation energy to the temperature (A/8), would give a maximum temperature T_{max} 7-8 MeV. With a more realistic level density parameter calculated at finite temperature (Bonche, 1984) (A/13) one gets $T_{max} \sim 10$ MeV. The experimental excitation energy per nucleon is smaller than ε_B. This might be related to the fact that the ebullition of a nucleus does not lead to a nucleon gas but to a mixture of nucleons and clusters. This is supported by the fact that clusters with a mass distribution porportional to $A_c^{-\tau}$ ($\tau \sim 7/3$), have been observed experimentally. This mass distribution can be tentatively interpreted, for instance, within the framework of a gas-liquid phase transition near the critical point (Minich, 1982), but other theoretical explanations, like a cold fragmentation (Bondorf, 1982) or a percolation phenomenon (Campi, 1985) are acceptable as well. Therefore, in the evaluation of ε^*, the maximum energy per nucleon that a nucleus can support before ebullition, one has to consider the following reaction mechanisms :

$$\text{Nucleus} \overset{(1)}{\rightleftarrows} \text{neutrons} + \text{protons} \overset{(2)}{\rightleftarrows} \text{clusters} \qquad (3)$$

which now correspond to a plethora of "boiled-off" neutrons, protons and clusters. It should be noted that all nucleons do not necessarily condensate in clusters. We shall not be interested in any theoretical justification of the $A_c^{-\tau}$ law but we shall use the fact that it is observed experimentally. In this case the most probable maximum energy content of a nucleus, expressed per nucleon, becomes :

$$\varepsilon^*_{max} = \varepsilon_B - \langle \varepsilon_{clusters} \rangle \qquad (4)$$

where $\langle \varepsilon_{clusters} \rangle$ is the mean binding energy per nucleon of the clusters. By using the most probable A_c mass value for a given cluster atomic number, together with a mass distribution in A_c, one finds $\langle \varepsilon_{clusters} \rangle \sim 3$ MeV. In Fig. 5 ε^*_{max} is plotted as a function of the mass A of the nucleus, for different values of the parameter τ. From Fig. 1 we see that medium nuclei can accomodate more excitation energy per nucleon than heavy nuclei. A compilation of the experimental data (Rivet, 1984) seems also indicate such a trend. It should be noted that the described calculation has to be considered only as semi-quantitative (see Leray, 1985). It is worth mentioning that the above evaluations assume that a global statistical equilibrium has been reached in the nucleus and that the upper limit on ε^*_{max} merely constitutes a most probable value, thus allowing for a certain amount of fluctuations. In particular, for cases where only "local equilibrium" is required one can doubtlessly exceed these limits and hence deposit energy locally in great excess of these ε^*_{max} values.
The purpose of the preceeding evaluation was to estimate ε^* and see if in Ar induced reactions one could get, in some cases, a limitation to incomplete fusion due to a too large amount of excitation energy. In (Leray, 1985) it has been shown that there is no limitation at 27 MeV/u and below, but such a limitation might exist at 35 and 44 MeV/u. Indeed, at these latter energies such a limitation exists for values which are of the order or greater than those given by eq.(1). Therefore, the maximum energy that one can deposit in a nucleus might truncate the ρ distribution and shift $\tilde{\rho}$ towards smaller values. The same calculation performed on the $^{12}C + ^{238}U$ and $^{20}Ne + ^{238}U$ systems show that ε^*_{max} begins to be reached at respectively 80-90 MeV/u and 50-60 MeV/u. This could explain why with ^{12}C and ^{20}Ne projectiles no such limitation has yet been observed.

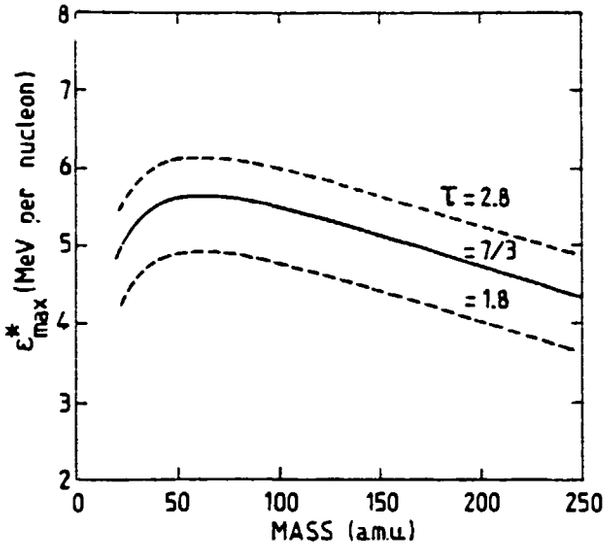

Fig. 5. Maximum energy per nucleon, for nuclei along the beta stability line, calculated assuming that clusters of mass A are formed with a probability $A^{-\tau}$. From (Leray, 1985).

CONCLUSION

The measurement of the most probable amount of LM transferred from the projectile to the fused system, $\tilde{p}$, provides a simple way to get informations about incomplete fusion. It depends not only on the bombarding energy but also on the size of the projectile and of the target. With Ar projectiles it has been found that above ~ 30 MeV/u a new regime was obtained. This transition might be related to the maximum energy that one can deposit in a nucleus under the condition of global statistical equilibrium.

REFERENCES

Ngo, C. (1985) to appear in Prog. in Part. and Nucl. and ref. therein.

Lefort, M., C. Ngô, J. Peter and B. Tamain (1973). Nucl. Phys. A216, 1766.

Siemssen, R.H. (1983). Nucl. Phys. A400, 245c and ref. therein.

Bondorf, J.P., J.N. De, G. Fai, A.O.T. Karniven, B. Jakobsson and J. Randrup (1980). Nucl. Phys. A333, 28 ; Robel, M.C. (1979). Ph.D. Thesis, Lawrence Berkeley Laboratory ; Davies, K.T.R., B. Rémaud, M. Strayer, K.R. Sandya Devi and Y. Raffray (1984). Ann. Phys. 156, 68 ; Leray, S., G. La Rana, C. Ngô, M. Barranco, M. Pi and X. Vinas (1985). Z. Phys. A320, 383.

Griffin, J.J. (1966). Phys. Rev. Lett. 17, 478 ; Blann, H. (1968). Phys. Rev. Lett. 21, 1357.

Sobel, M.I., P.J. Siemens, J.P. Bondorf and H.A. Bethe (1975). Nucl. Phys. A251, 502 ; Weiner, R. and M. Westrom (1977). Nucl. Phys. A286, 282.

Grégoire, C. and B. Remaud (1983). Phys. Lett. B127, 308 ; Tricoire, H (1984). Thèse de Doctorat d'Etat, Orsay.

Sikkeland, T (1968). Phys. Lett. 27B, 277.

Viola, V.E., B.B. Back, K.L. Wolf, T.C. Awes, C.K. Gelbke and H. Breuer (1982). Phys. Rev. 26C , 178.

Saint-Laurent, F., M. Conjeaud, R. Dayras, S. Harar, H. Oeschler and C. Volant (1982). Phys. Lett. 110B, 372.

Galin, J., H. Oeschler, S. Song, B. Borderie, M.F. Rivet, I. Forest, R. Bimbot, D. Gardès, B. Gatty, H. Guillemot, M. Lefort, B. Tamain and X. Tarrago (1982). Phys. Rev. Lett. 48, 1787.

La Rana, G., G. Nebbia, E. Tomasi, C. Ngô, X.S. Chen, S. Leray, P. Lhenoret, R. Lucas, C. Mazur, M. Ribrag, C. Cerruti, S. Chiodelli, A. Demeyer, G. Guinet, J.L. Charvet, M. Morjean A. Péghaire, Y. Pranal, L. Sinopoli and J. Uzureau (1983). Nucl. Phys. A407, 233.

Leray, S., G. Nebbia, C. Grégoie, G. La Rana, P. Lhénoret, C. Mazur, C. Ngo, M. Ribrag, E. Tomasi, S. Chiodelli, J.L. Charvet and C. Lebrun (1984). Nucl. Phys. A425, 345.

Charvet, J.L., S. Chiodelli, C. Grégoire, C. Humeau, G. La Rana, S. Leray, P. Lhénoret, J.P. Lochard, R. Lucas, C. Mazur, M. Morjean, C. Ngô, Y. Patin, A. Péghaire, M. Ribrag, S. Seguin L. Sinopoli, T. Suomijarvi, E. Tomasi and J. Uzureau (1982). Int. Conf. on theoretical approach to heavy ion reaction mechanisms, Paris, p. 82.

Leray, S., D. Granier, C. Ngo, E. Tomasi, C. Cerruti, P. Lhénoret, R. Lucas, C. Mazur, M. Ribrag, J.L. Charvet, C. Humerau, J.P. Lochard, M. Morjean, Y. Patin, L. Sinopoli, J. Uzureau, D. Guinet, L. Vagneron and A. Peghaire (1985). Z. Phys. A320, 533 and XXIII Inter. Winter Meeting on nuclear physics, Bormio (1985).

Jacquet, D., J. Galin, B. Borderie, D. Gardès, D. Guerreau, M. Lefort, F. Monnet, M.F. Rivet, X. Tarrago, E. Duek and J.M. Alexander (1985). Preprint, Orsay, IPNO-DRE-85-09.

Cerruti, C. (1983). Thèse de Doctorat d'Etat, Lyon ; Cerruti, C., D. Guinet, S. Chiodelli, A. Demeyer, K. Zaïd, S. Leray, P. L'Hénoret, C. Mazur, C. Ngô, M. Ribrag, A. Lheres, submitted to Nucl. Phys.

Borderie, B., M.F. Rivet, C. Cabot, D. Fabris, D. Gardès, H. Cauvin, F. Hanappe,, and J. Peter (1984). Preprint, Orsay, IPNO-DRE-84-13.

Ngo, C., D. Dalili and R. Lucas (1985). XXIII Inter. Winter Meeting on nuclear Physics, Bormio.

Boncne, P., S. Levit and D. Vautherin (1984). Nucl. Phys. A427, 278.

Rivet, M.F. and B. Borderie (1984). Tsukuba Inter. Symp. on heavy ion fusion reactions, Japon.

Minich, R.W., S. Agarwal, A. Bujak, J. Chuang, J.E. Finn, L.J. Gutay, A.S. Hirsh, N.T. Porile, R.P. Scharenberg, B.C. Stringfellon and F. Turkot (1982). Phys. Lett. 118B, 458.

Bondorf, J.P. (1982). Nucl. Phys. A387, 25c ; Aichelin, J., J. Hüfner and R. Ibarra (1984). Phys. Rev. C30, 107 ; Aichelin, J. and J. Hüfner (1984). Phys. Lett. 136B, 15.

Campi, X. and J. Desbois (1985). XXIII Inter. Winter Meeting on nuclear physics, Bormio and ref. therein.

NUCLEAR CALEFACTION

C. Ngô, D. Dalili, R. Lucas, C. Cerruti*, S. Leray, C. Mazur, M. Ribrag, T. Suomijarvi and M. Berlanger

Service de Physique Nucléaire - Mesures Fondamentales
CEN Saclay, 91191 Gif-sur-Yvette Cedex, France

S. Chiodelli, A. Demeyer and D. Guinet

IPN Lyon, Université Claude Bernard Lyon 1
69622 Villeurbanne Cedex, France

*on leave from IPN Lyon

INTRODUCTION

At low bombarding energies (E/A < 10 MeV/u) the fusion of two nuclei is possible provided the product, Z_1Z_2, of their atomic number is not too large (Ngô) (typically when $Z_1Z_2 \leq 2500$-3000). With argon projectile or lighther ones the small impact parameters lead to fusion and the large ones, corresponding to grazing collisions, lead to quasi-elastic or inelastic reactions. A small bin of impact parameters located between those giving fusion and those correspond to grazing collisions lead to deep inelastic collisions. With these projectiles the fusion cross section represents always a large part of the total reaction cross section. It has been shown (Lefort, 1973) that this is no longer the case with projectiles like Kr or heavier on heavy targets and the fusion cross section becomes vanishingly small. This is due to the coulomb force between the two interacting nuclei which becomes so strong that it cannot be counteracted by the nuclear force (Ngô, 1975). As a consequence fusion is no longer possible and the impact parameters which were expected to give fusion lead to deep inelastic phenomenon which occurs with a cross section which is now a large part of the total reaction cross section.

When the bombarding energy is raised above ~ 20 MeV/u we have seen, in the first lecture, that incomplete fusion replaces progressively complete fusion when projectiles like Ar or lighter are involved. With Kr ions, or heavier ones, and heavy targets the coulomb force between the two nuclei has the same strenght as at low bombarding energy. Consequently, it is reasonable to think that incomplete fusion will not be very probable in Kr induced reactions on heavy targets. The question is to know which mechanism will replace it. In this lecture we shall try to give an answer to this question using the results of a recent experiment performed at GANIL with Kr projectiles. A preliminary experimental investigation on the Kr + Au system at 35 MeV/u has indeed shown the existence of products with an atomic number, Z, and a kinetic energy, E, substantially smaller than the one of the projectile (Dalili, 1984). Typically, events with Z ~ 25 and E/A ~ 15-20 MeV/u have been detected. More detailed studies concerning this subject have been obtained on the $^{84}Kr + {}^{92}Mo$, ^{98}Mo, $^{nat.}Ag$ and ^{197}Au systems at 22 MeV/u (Dalili, 1985; Dalili, 1985). We shall present an overview of these results in section 1. In section 2 we shall propose a simple interpretation of the energy-relaxed products observed in these collisions. We shall see that they could possibly come from a calefaction type phenomenon.

I. OVERVIEW OF THE EXPERIMENTAL RESULTS

The $^{84}Kr + {}^{92,98}Mo$, ^{Nat}Ag and ^{197}Au systems have been investigated using the 22 MeV/u Kr beam accelerated at GANIL. The atomic number Z, the mass A and the kinetic energy E of the products have been measured between 6° and 12° in the laboratory system. In this lecture we shall only present some of the results obtained in (Dalili, 1985).
In the discussion it should always be kept in mind that the grazing angle, θ_{gr}, associated with the projectile is respectively equal to 6°, 7° and 10° for the Kr + Mo, Kr + Ag and Kr +

Au systems. Therefore, we are a little bit beyond it for the Kr + Mo systems whereas θ_{gr} is within the detection angular range for the two other reactions. In Fig. 1 the velocity spectrum of the products is displayed for different laboratory angle (bins of ± 0.5° around the indicated value). The projectile velocity is equal to 6.5 cm/ns and indicated by an arrow. Low inelasticity products (elastic, quasi-elastic, fragmentation,...) have a velocity close to the projectile one and are mainly observed at angles smaller than θ_{gr}. For a given system, as one moves to large detection angles, the amount of low inelastically events decreases and, beyond the grazing angle, one is left with products which have a velocity distribution peaked around 4-5 cm/ns. In Fig. 2 the atomic number distributions of the products is shown for different values of the laboratory angle. Products corresponding to a low inelasticity are focused in the region corresponding to Z=36 which is the atomic number of the projectile. As one moves to detection angles larger than the grazing angle one observes a broad distribution peaked at about Z ~ 20-25 units.

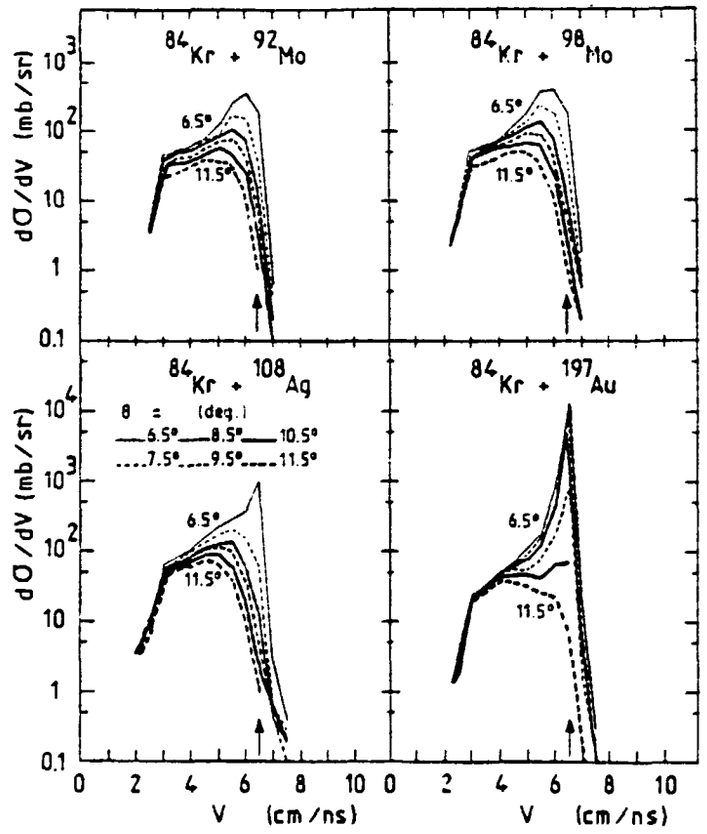

Fig. 1. Velocity spectra of the products detected in the Kr + ^{92}Mo, Kr + ^{98}Mo, Kr + ^{nat}Ag and Kr + ^{197}Au reactions at 22 MeV/u plotted for several bins of angles.

In Fig. 3 the atomic number distributions of the products, integrated over the detection angular range, is displayed for different bins of kinetic energies. As the inelasticity increases the distribution broadens and, at the same time, the most probable Z value decreases. Another way to view the results is displayed in Fig. 4 where the kinetic energy distribution of the products, integrated over 6-12°, is plotted for different atomic numbers and for the four investigated systems. Again, one observes two components for Z values close to the one of the projectile which merge progressively as the atomic number decreases.
It is now established that products with a low kinetic energy and a mass substantially smaller than the one of the projectile are formed in krypton induced reactions at bombarding energies energies around 20-40 MeV/u. These products are mostly visible at angles larger than θ_{gr} because low inelastically products have almost disappeared there. However, it is important to note that they are also present at smaller angles. The purpose of the next section will be to propose a possible explanation for the formation of these events.

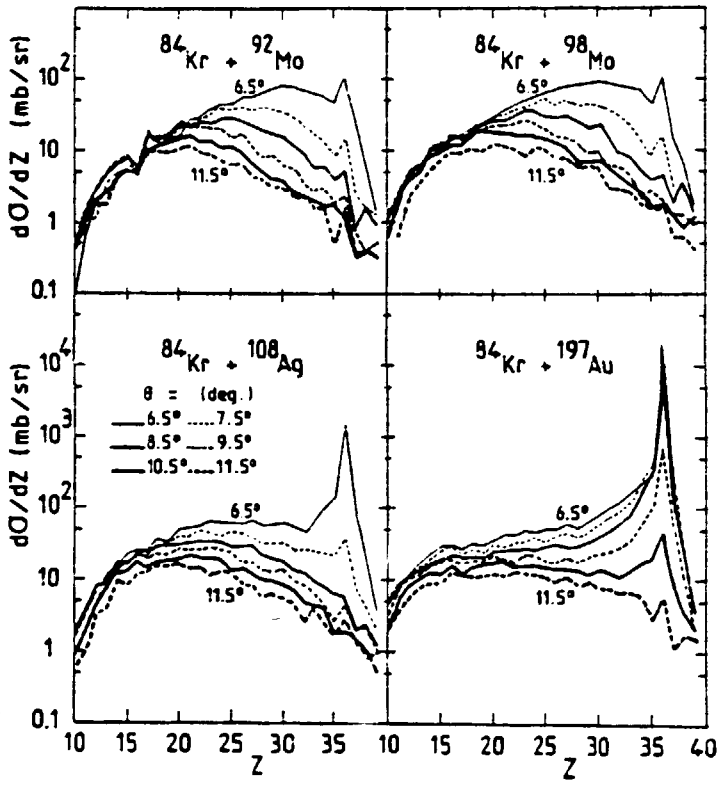

Fig. 2. Atomic number distributions for several bins of angles and for the four investigated systems.

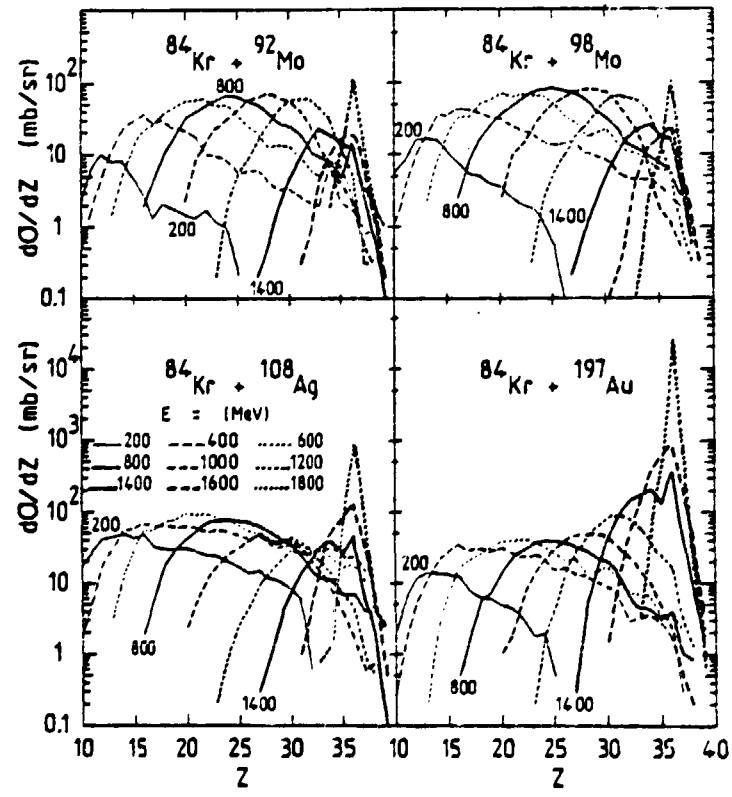

Fig. 3. Atomic number distributions of the reaction product detected between 6° and 12° for different bins of kinetic energies (each bin correspond to ± 100 MeV around the indicated value.

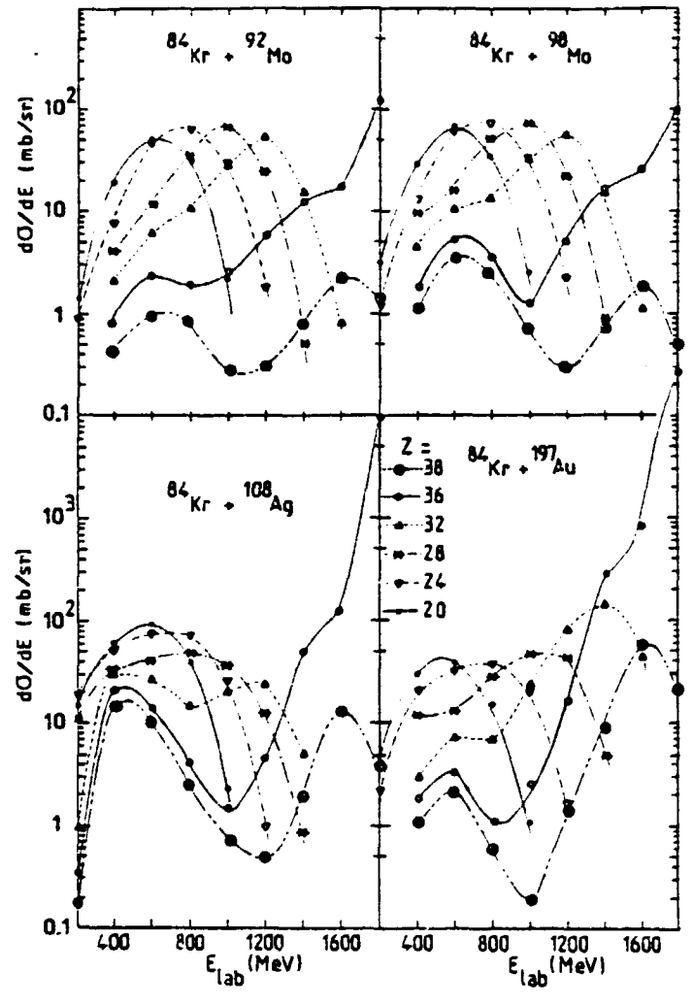

Fig. 4. Kinetic energy distributions for different values of the atomic numbers and for the 4 investigated systems.

II. CALEFACTION PHENOMENON

We shall now propose a very schematic interpretation of the preceeding measurements concerning the unexpected observed events. This interpretation is tentative since the experimental results are inclusive. Nevertheless, it can be used as a basis for future experiments. In such heavy ion reactions one is faced with products which can be highly excited. Since one detects the reaction products after their de-excitation it is necessary to take into account this process when discussing the experimental data. We have made a very simple treatment of the de-excitation process by treating the evaporation sequence as a continuous process (see (Dalili, 1985) for more details). Such a treatment is of course approximate but it will be sufficient for our discussion. We shall now make several hypotheses for the reaction mechanisms and check which one is in best agreement with the experimental data.

a) Deep inelastic reactions

The first idea would be to extrapolate our knowledge at low bombarding energy and suppose that the observed energy relaxed products are coming from a deep inelastic collisions (Lefort, 1978). However, in this case one would rather expect a mass transfer from the projectile to the target rather than the opposite. The drift in the other direction which one observes in the present experiment could perhaps be understood as the result of the evaporation of highly excited deep inelastic fragments. To check this hypothesis we have assumed that there is no

mass drift in the deep inelastic process in order to maximize the evolution of the secondary products towards small masses. In Fig. 5 is displayed the calculated correlation between the most probable mass and kinetic energy of the products expressed in dimensionless units (A_p and E_p are the mass and the kinetic energy of the projectile respectively). The products before evaporation (primary products) correspond to $A/A_p = 1$ according to our assumption. The secondary products (after evaporation) are represented by the dasned lines (here and in the following we shall restrict ourselves to two systems : $^{84}Kr + ^{98}Mo$ and ^{197}Au). One sees that the evaporation process changes a lot the primary correlation. Indeed, in some cases one third of the initial mass is evaporated. In Fig. 5 one has also plotted the most probable values corresponding to each of the peaks observed experimentally and shown in Fig. 4. A quick comparison between the calculated and the experimental results indicates that it would be difficult to explain the whole set of data by a deep inelastic process followed by evaporation.

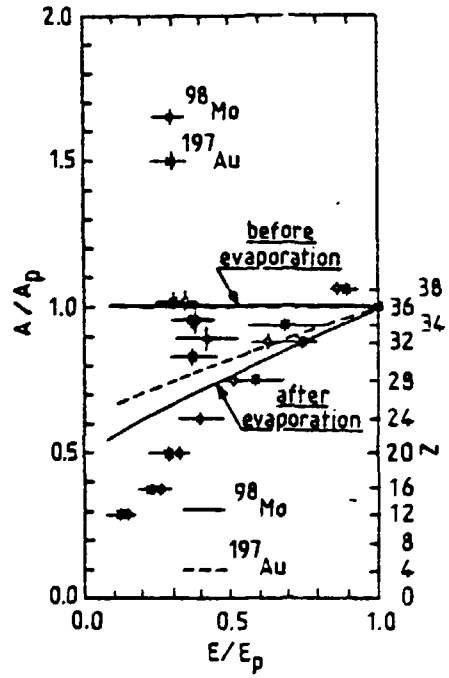

Fig. 5. The calculated correlation between the mass A (in units of the projectile mass) and the kinetic energy (in units of the incident energy) are plotted for the most probable products obtained in the $^{84}Kr + ^{98}Mo$ and $^{84}Kr + ^{197}Au$ reactions before and after evaporation, assuming a deep inelastic process. The left hand side graduation corresponds to the atomic numuer Z. In this Fig. one also shows experimeal points deduced from the most probable values of the distributions displayed in nows Fig. 4. The horizontal bars, for the Kr + Au data, correspond to the standard deviation of the associated distribution.

b) The participant-spectator picture

The participant-spectator picture has been very successful at higher bombarding energies (Bowan, 1975) and one might see wether it is still applicable at 22 MeV/u. In this picture one distinguishes three kinds of events which move at different velocities. Each of them is associated with one of the following interaction zone : the projectile spectators (PS) region which moves with the projectile velocity, the target spectators (TS) at rest in the laboratory system, and the participants domain (PD) moving with an intermediate velocity. A similar comparison as the one done in Fig. 5 can be performed and is shown in Fig. 6. It shows that the participants-spectators picture does not apply very well. However, it should be noted that the qualitative evolution of the experimental data is not so badly reproduced.

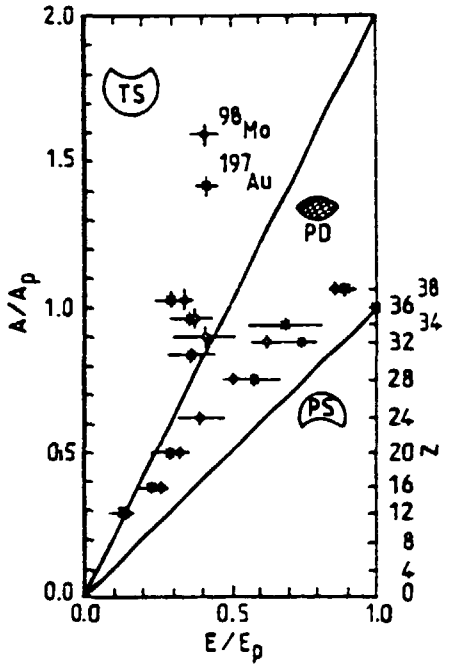

Fig. 6. Same as fig. 5 assuming the participants-spectators picture. Here, the secondary products corresponding to PS lie on the same locus as the primary ones because the average velocity is conserved in the evaporation process. The TS zone is only little excited and consequently the primary and the secondary correlations are the same.

c) The role of the mean field

It might not be too surprising that the models which were very successful at low and high bombarding energies do not apply so well between 20 and 50 MeV/u. Indeed, in this energy range one expects the mean field and the individual nucleon nucleon interactions to play a significant role in the reaction mechanisms. We shall now investigate, in a qualitative way, what could be the influence of the mean field on a participants-spectators picture which was the framework which gave the best qualitative agreement with the experimental data.
The role of the mean field in a participants-spectators picture is to favor the fusion between some or all of the three pieces (PS, TS and PD) created during the interaction. The simplest interaction is of course the one where the 3 pieces fuse after some particles have been emitted by the participant zone. Such a mechanism would correspond to incomplete fusion and might be what happens with lighter projectiles. However, with krypton ions we have already said that the coulomb interaction will prevent such a mechanisms to occur. Therefore, one can imagine any of the alternative interaction scenarios described below.

1. Partial fusion and thermalization

One can imagine that the participant zone fuses with either the projectile or the target spectators, two hypothetical scenarios schematically represented in the left part of Fig. 7 (Fig. 7b and 7d). In Fig. 7b one would be dealing with the (PS + PD) agregate (in Fig. 7d with the (TS + PD) one) moving as a single system. The excitation energy of the participants could then be shared with the spectators of either the projectile (Fig. 7b) or of the target (Fig. 7d) to the extend that a highly excited nucleus is formed which, most probably, will fission. As we did in Fig. 5 and 6 one can calculate the correlation between the mass and the kinetic energy of the different fragments produced in the reaction. This is shown in the middle and in the right part of Fig. 7 for the products before and after evaporation.

2. Partial fusion and calefaction

One could also suppose that the mean field induces, at first, the same mechanisms as above, namely the PD fuse with either the PS or TS zones (Fig. 7a and 7c). However, and this constitute the crucial difference, the fused system does not live long enough to get uniformly excited but breaks up before a final global equilibrium is achieved. The reseparation of the fused system could be attributed to "calefaction", a phenomenon well known in the case of macroscopic systems. For instance, one knows that pouring some water over an overheated plate results in a "calefaction" of the water droplets. The mechanism can be explained as a slower than expected liquid to vapor transition for the water content of the droplets. The vapour layers, developped upon contact with the heated plate, tends to isolate the remnants of the water droplets from the heat source because it has a lower thermal conductivity than the water itself. A similar mechanism also allows one to put one's hand in liquid nitrogen without suffering any serious damage, provided it is done fast enough.
For heavy ion collisions one surmises that a nucleons gas, generated by the initial evaporation of the hot zone or from overheating of the spectator zone, fills the contact region between the participants and the spectators of the combined (PD + PS) or (PS+ TS) systems (see Fig. 7a and 7c). Such a nucleon gas is expected to have a smaller thermal conductivity than the corresponding region of participants matter which would have both a higher nucleon density and temperature. Therefore, calefaction phenomenon will allow a reseparation of the fused system into its participants and spectators constituents. The calculated correlation between A and E is shown in the middle and in the right part of Fig. 6.

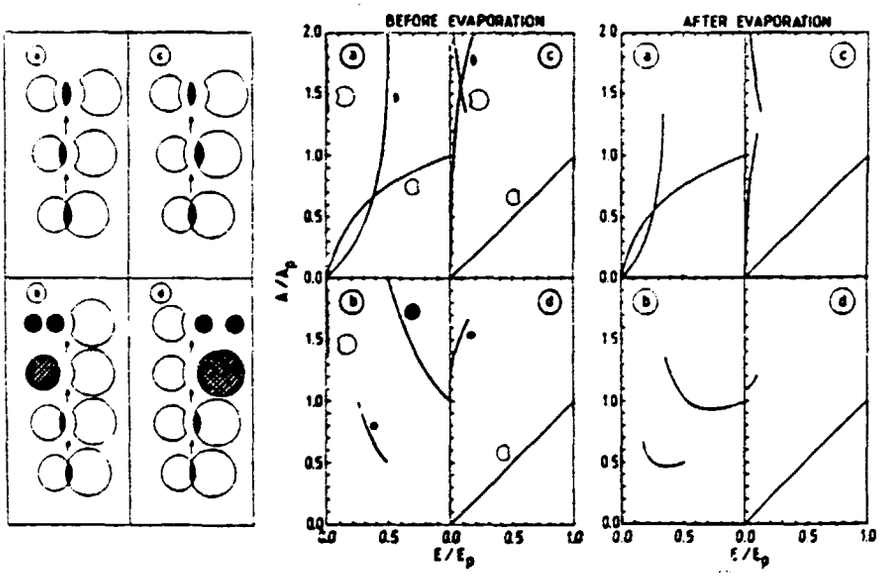

Fig. 7. Four different mechanisms, derived from the participants-spectators picture assuming that the mean field still play a role, are schematically displayed in the right hand part of the figure. In the middle of the figure, one shows the calculated correlation $(A/(A_p), E/(E_p))$ for the primay products corresponding to each of the four scenarios. The left hand part of the figure shows the calculated correlations after evaporations.

3. Conclusion : calefaction?

As we did in Fig. 5 and 6 one can compare the calculated correlations with the experimental results. It turns out that only the scenario corresponding to Fig. 7a (calefaction phenomenon in the (PD + PS) system) could possibly fit the datas. The comparison is displayed in Fig. 8 where the calculated correlation of the primary products (full line) as well as the corresponding one after evaporation (dashed) line are shown. It should be noted that the projectile spectators are hardly excited. Therefore, the correlation of the secondary products is the same. Compared to the usual participants-spectators model, it should be stressed that in the calefaction picture the PD and the PS zone move with practically the same velocity which is by far not the case in the other model.

The present description is of course very schematic and we refer the reader to (Dalili, 1985) for more details, especially concerning a more thorough discussion of the different mechanisms.

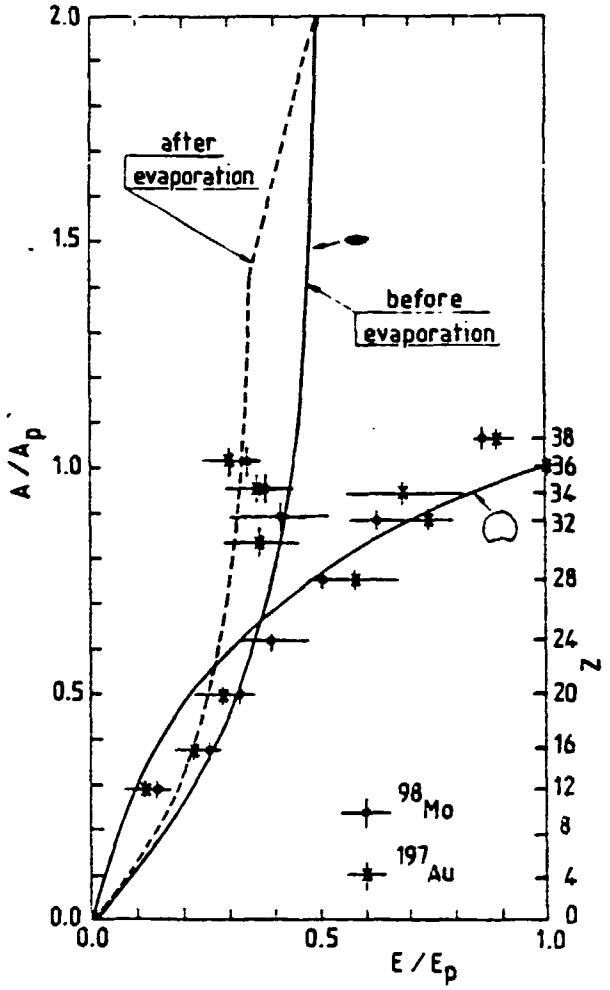

Fig. 8. A comparison between the experimental data the calculated correlation for scenario a of figure (calefaction in the PS + PD system) is displayed is in Fig. 5 and 6.

CONCLUSION

We have described some recent results obtained at GANIL with krypton projectile at 22 MeV/u on medium and heavy targets. It was found, in the 6-12° angular range, products with an atomic number, a mass and a kinetic energy substantially smaller than the one of the projectile. It appeared difficult to interpret these results in terms of a deep inelastic process or within the usual participants-spectators picture. It was proposed that they could be produced in a mechanism where one has first a partial fusion between the participants and the projectile spectators followed by a reseparation of these two pieces due to a *calefaction phenomenon*. At variance to the usual participants-spectators model the two pieces coming from the reseparation of the partial fused system have practically the same velocity.
Such an hypothesis is not in contradiction with the inclusive datas. However, coincidence experiments are now really needed in order to completely check the proposed hypothesis of calefaction. This phenomenon seems to be a characteristics of Kr induced reactions with medium and heavy targets. Indeed, in a recent experiment performed at GANIL with Xe ions at 24 MeV/u, it seems that we have observed also similar products. With lighter ions like Ar, or lighter ones, this phenomenon might exist as well but probably with a much smaller probability (indeedone has still the incomplete fusion mechanism which exhaust, in many cases, a large part of the total reaction cross section). The differences between light and heavy projectiles

might be due to the coulomb force a situation very similar, in that respect, to the one we know at lower bombarding energies.

REFERENCES

Ngô, C. Prog. in part and nucl, in press and ref. therein.

Lefort, M., C. Ngô, J. Peter and B. Tamain (1973). Nucl. Phys. A216, 166.

Ngô, C., B. Tamain, J. Galin, M Beiner and R.J. Lombard (1975). Nucl. Phys. A240, 353.

Dalili, D., P. L'Hênoret, R. Lucas, C. Mazur, C. Ngô, M. Ribrag, T. Suomijarvi, E. Tomasi, B. Boishu, A. Genoux-Lubin, C. Lebrun, J.F. Lecolley, F. Lefebvres, M. Louvel, R. Regimbart, J.C. Adloff, A. Kamili, G. Rudolf and F. Scheibling (1984). Z. Phys. A316, 371.

Dalili, D., R. Lucas, C. Ngô, C. Cerruti, S. Leray, C. Mazur, M. Ribrag, T. Suomijarvi, M. Berlanger, S. Chiodelli, A. Demeyer and D. Guinet (1985). Preprint DPhN/Saclay n°2255.

Dalili, D., M. Berlanger, S. Leray, R. Lucas, C. Mazur, C. Ngô, M. Ribrag, T. Suomijarvi, C. Cerruti, S. Chiodelli, A. Demeyer, D. Guinet, A. Genoux-Lubin, C. Lebrun, J.F. Lecolley, F. Lefebvres and M. Louvel (1985). Z. Phys. A320, 349.

Lefort, M., and C. Ngô (1978). Ann. Phys. (Paris) 3, 5 and ref. therein.

Bowan, J.D., W.J. Swiatecki and C.F. Tsang (1975). LBL Report n°29098. Westfall, G.D., J. Gosset, P.J. Johansen, A.M. Poskanzer, W.G. Meyer, H.H. Gutbrod, A. Sandoval and R. Stock (1976). Phys. Rev. Lett. 37, 1202.

MECHANICAL INSTABILITY OF HOT AND COMPRESSED NUCLEI INVESTIGATED IN THE FRAMEWORK OF A SPHERICAL TIME DEPENDENT THOMAS-FERMI APPROACH

J. Nemeth*, C. Ngô and E. Tomasi
Service de Physique Nucléaire - Métrologie Fondamentale
CEN Saclay, 91191 Gif-sur-Yvette Cedex, France

and

M. Barranco
Fisica Atomica i nuclear, Universitad de Barcelona
Diagonal 645, Barcelona 28, Spain

*Permanent address : Eötvos University, Budapest, Hungary

The Hartree-Fock approximation has been very successful to calculate static properties of nuclei (Quentin, 1979). It is a mean field approximation to the many body problem where the many body wave function is approximated by a slater determinant built on single particle wave functions. Besides static calculations, the time dependent Hartree-Fock (TDHF) method has been successfully applied at low bombarding energies heavy ion reactions (Bonche, 1976). It has provided a good quantitative description of the collision of two nuclei. In particular, fusion and deep inelastic reactions have been mocked up by this method in a reasonable way. One of its great advantages is to be a self consistent theory which can be deduced from a variational principle which makes the "action" :

$$\mathcal{A} = \int_{t_1}^{t_2} dt \, \langle \Psi(t) | i\hbar \frac{\partial}{\partial t} - \hat{H} | \Psi(t) \rangle \qquad (1)$$

stationary with respect to a variation of the single particle wave function ϕ_k. Here, H is the hamiltonian and Ψ a slater determinant built from the ϕ_k. All the calculations performed so far have been done at temperature zero but one knows that deep inelastic collisions and fusion reactions lead to nuclei at finite temperature. The heating up of these nuclei cannot be reproduced by a TDHF calculation. Furthermore, it is a non dissipative theory since the entropy of the system is conserved whereas one knows that it should increase in these processes. The above shortcomings of the TDHF approach are due to the fact that two body collisions are neglected. However, it is these two body and higher order collisions which are responsible for the decay of 1 particle - 1 hole excitations to more complicated states (temperature). Therefore, a realistic treatment of dissipative heavy ion collisions needs to go beyond the TDHF approximation. At bombarding energies between ~ 20-50 MeV/u nuclei can be formed at much higher temperature values and it becomes necessary to take care explicitly of this parameter. Furthermore, two body collisions become more and more important as the bombarding energy increases because the Pauli blocking effect decreases. These two body collisions can be a source of dissipation which has to be taken into account. At finite temperature shell effects are progressively washed out and semiclassical approximations become good enough to be applied with a reasonable amount of confidence (Brack). In this lecture we shall present a time dependent Thomas-Fermi (TDHF) (Nemeth, 1985) approach which is a first step in trying to understand the dynamical evolution of highly excited nuclei. In section I we shall briefly sketch the formalism. The method will then be applied, in a one dimensional case, to investigate the evolution of hot and compressed nuclei.

I. FORMALISM

One way to derive the TDTF equations is to start from the TDHF approach and extend the derivation at finite temperature including eventually dissipation in a phenomenological way.
Let us first start by considering the temperature T=0 case in order to see the connection between the TDTF and the TDHF approaches. With a phenomenological density dependent effective interaction, like those of the Skyrme type (Quentin, 1979), eq.(1) can be rewritten as :

$$\mathcal{A} = \int_{t_1}^{t_2} dt \int d\vec{r} \sum_{k,\alpha} i \phi_k^{(\alpha)*} \dot{\phi}_k^{(\alpha)} + \frac{\hbar^2}{2m} \phi_k^{(\alpha)*} \Delta\phi_k^{(\alpha)} - W(\rho_n,\rho_p) \qquad (2)$$

Where $W(\rho_n,\rho_p)$ is the potential energy density which depends on the neutron and proton densities (ρ_n,ρ_p) and m the nucleon mass. The superscript α stands either for neutrons (α=n) or for protons (α=p). In eq.(2) a dot above a variable denotes the time derivative operator. By varying eq.(2) with respect to ϕ_k or ϕ_k^* one gets the TDHF equations :

$$i\hbar \dot{\phi}_k^{(\alpha)} = -\frac{\hbar^2}{2m} \Delta\phi_k^{(\alpha)} + U^{(\alpha)} \phi_k^{(\alpha)} \qquad (3)$$

where $U^{(\alpha)}$, the single particle potential, is the functional derivative of W with respect to the α density.
Without introducing any approximation one may write the single particle wave function $\phi_k^{(\alpha)}$ as :

$$\phi_k^{(\alpha)} = \phi_k^{(\alpha)} e^{iS_k^{(\alpha)}} \qquad (4)$$

where both $\phi_k^{(\alpha)}$ and $S_k^{(\alpha)}$ are reals. The quantity $\hbar/m\ \nabla S_k^{(\alpha)}$ has a very simple physical semi classical meaning : it is just the velocity of the particle in the k orbit. One way to introduce the TDTF approximation is to suppose that all the phases $S_k^{(\alpha)}$ are locally the same for each kind of nucleons ($S_k^{(\alpha)} = S^{(n)}$ for neutrons and $S_k^{(\alpha)} = S^{(p)}$ for protons). This amounts to say that the neutrons or the protons have locally all the same velocity. Using this approximation one can rewrite the action as :

$$\mathcal{A} = \int_{t_1}^{t_2} dt \int d\vec{r} \sum_{\alpha=n,p} -\left(\hbar \dot{S}^{(\alpha)} \rho_\alpha + \frac{\hbar^2}{2m} \rho_\alpha (\nabla S^{(\alpha)})^2 + e[\rho_\alpha] \right) \qquad (5)$$

where $e[\rho_\alpha]$ is the energy density per unit volume of the system. Varying $\mathcal{A}$ given by eq.(5) with respect to ρ_α and $S^{(\alpha)}$ gives the TDTF equation at zero temperature. These equations are a semiclassical approximation of the TDHF ones. However, it is easy to extend eq.(5) at finite temperature by replacing the energy density $e[\rho_\alpha]$ by the free energy density $f[\rho_\alpha]$. This will allow to treat finite temperature effects, a task which would be much more difficult to do within the framework of a TDHF approach. The TDTF equations obtained in this way read :

$$-\hbar \dot{S}^{(\alpha)} = T\, n_\alpha + U^{(\alpha)} + \frac{\hbar^2}{2m} (\nabla S^{(\alpha)})^2 \qquad (\alpha = n,p) \qquad (6)$$

$$-\frac{\hbar}{2} \dot{\rho}_\alpha = \frac{\hbar^2}{2m} \nabla(\rho_\alpha \nabla S^{(\alpha)}) \qquad (\alpha = n,p) \qquad (7)$$

where n_α is the degeneracy parameter entering in the usual definition of ρ (see Dalili) and $U^{(\alpha)}$ the single particle potential associated with the neutrons or protons. This latter term includes some kinetic energy corrections which go beyond the usual Thomas-Fermi approximation. The physical meaning of eq.(6) and (7) is the following : eq.(7) is just a continuity equation. If one takes the gradient of both sides of eq.(6) and remembers that $\hbar/m\ \nabla S^{(\alpha)}$ is the velocity field of particles α, one gets an Euler-like hydrodynamics equation. Therefore, the TDTF equations presented in eq.(6) and (7) are just fluid dynamical equations.
The TDTF equations are non homogeneous which makes their numerical resolution rather tricky. However, by an appropriate transformation one can get equations which can be more easily solved numerically. Indeed, it has been shown (Dalili; Levit, 1984) that static Thomas-Fermi equations can be solved in the same way as Hartree-Fock equations by introducing two "virtual" wave functions (one for protons and the other for neutrons) $\chi_\alpha = \sqrt{\rho_\alpha}$. This can be extended to the time dependent case (Nemeth, 1985) by introducing :

$$\chi_\alpha = \sqrt{\rho_\alpha}\ \exp(iS^{(\alpha)}) \qquad (8)$$

then eq.(6) and (7) lead to :

$$i\hbar \dot{\chi}_\alpha = -\frac{\hbar^2}{2m} \Delta\chi_\alpha + (T\, n_\alpha + V^{(\alpha)})\ \chi_\alpha \qquad \alpha = n,p \qquad (9)$$

where

$$V^{(\alpha)} = U^{(\alpha)} + \frac{\hbar^2}{2m} \frac{\Delta\rho_\alpha^{1/2}}{\rho_\alpha^{1/2}} \qquad (10)$$

Therefore, the 4 fluid dynamical equations (eq.(6) and (7) for α = n,p) are equivalent to the 2 "Schrödinger" equations (eq.(9) for α = n,p). It should be noted that the total number of equations is conserved since χ_α are complex functions whereas ρ_α and $S^{(\alpha)}$ are reals. Eq.(6) has the same mathematical structure as a TDHF equation and all the powerful numerical methods developped in this field can be used.
During the time evolution of the system the temperature will change. For instance a gas in expansion cools down. In the applications described in this lecture we shall restrict ourselves to the case where one assumes a global statistical equilibrium over the entire system. This means that, at a given time, the temperature will be the same throughout the whole nucleus. Such a situation is very likely to be found in heavy ion collisions at bombarding energies < 50-100 MeV/u. In this case, the evolution of the temperature as a function of time can be obtained from the total energy conservation.
It should be stressed that eq.(9) is just a convenient way to solve the fluid dynamical eq.(6) and (7) but introduces in no way new physics.
The TDTF framework also allows to simulate the effect of two body collisions by introducing a phenomenological friction term in the dynamical equations of motion. This friction will allow to convert the energy which is in the velocity field (collective energy) into intrinsic excitation (heat). A possible way to do that is to make an analogy with the Navier-Stockes equations in hydrodynamics and modify eq.(6) in the following way :

$$-\hbar \dot{S}^{(\alpha)} = T\,\eta_\alpha + U^{(\alpha)} + \frac{\hbar^2}{2m}\nabla S^{(\alpha)})^2 - \gamma\,\frac{\hbar}{m}\nabla(\rho_\alpha \nabla S^{(\alpha)}) \qquad (11)$$

where the last term is a phenomenological dissipative one. γ is the friction coefficient including a proper form factor. With this modification of the Euler equation, the dynamical evolution of the system will be of dissipative nature with an increase of the entropy per unit of time equal to

$$\sum_\alpha \gamma\,\frac{\hbar^2}{m^2}\,[\nabla(\rho_\alpha\, S^{(\alpha)})]^2$$

II. RESULTS

The TDTF approach was used to investigate the stability of hot and compressed nuclei in global statistical equilibrium. Their evolution was followed over a time scale of the order of a few 10^{-22}s which corresponds typically to the interaction times in heavy ion induced collisions at bombarding energies ~ 20-50 MeV/u. The calculation is self consistent but we have restricted ourselves to the one dimensional case where nuclei are assumed to keep spherical symmetry during their evolution.

a) Compressional energy versus thermal excitation

In heavy ion collisions induced at bombarding energies between ~ 20 and 50 MeV/u energy can be deposited in two extreme forms : compressional energy which is of collective nature and thermal excitation (heat) which is on the contrary desorganized. In order to investigate the influence of these two different kinds of excitation on the future evolution of the nuclei we have used, for the initial conditions of the TDTF calculations, nuclei obtained as the result of a static, finite temperature, self consistent Thomas-Fermi calculation with a constraint on the mean square radius $\langle r^2\rangle$. It means that the initial configuration has been obtained by minimization of the quantity $F + \lambda \langle r^2\rangle$, where F is the total free energy and λ the Lagrange multiplier associated with $\langle r^2\rangle$. Here, λ is a measure of how much the system is compressed (it gives a velocity field proportional to $\vec{r}$ (monopole constraint), whereas the temperature T is related to its thermal excitation.
In Fig. 1 we show the time evolution of the density profile corresponding to a ^{208}Pb nucleus plotted as a function of the radial distance r, for different values of T and λ. For λ = 0.2 MeV/fm^2 and T=0, 3 and 5 MeV, one observes that the density oscillates around an equilibrium value. This can be viewed as a rather large amplitude monopole vibration. For these 3 cases the nucleus remains stable for times of the order of a few 10^{-22}s. This is no longer the case if one compresses the nucleus too much as is can be seen from the right hand side (RHS) of Fig. 1 for λ = 0.4 MeV/fm^2. Here one observes for T = 0.3 and 5 MeV that, as the time goes on, the surface region separates from the center thus forming a kind of "bubble nucleus". At the same time the system cools down (if T ≠ 0) and the nucleus becomes unstable under high compression and finally "blows up" (~ 2×10^{-2}s). One should not pay too much attention to the bubble nuclei which are very likely obtained because of the imposed spherical symmetry.

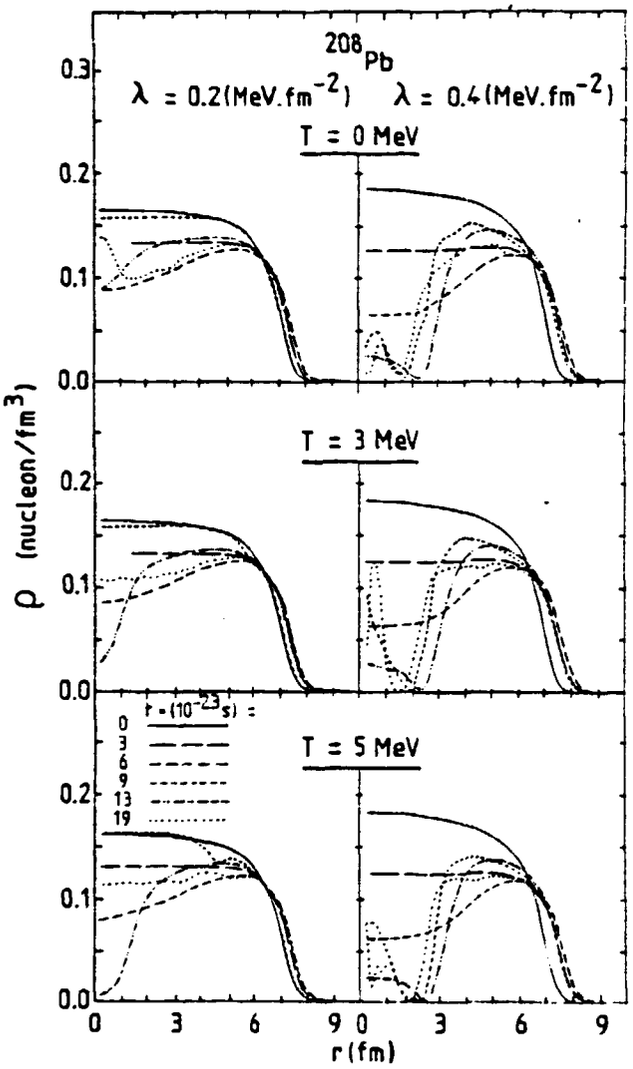

Fig. 1 Six sequential density profiles of ^{208}Pb, represented by a different graph for instants t=0, 6, 12, 18, 26 and 19 x 10^{-22}s, plotted against the nuclear radius, r, for three different T and two λ values. Calculations were performed in a 40 fm radius spherical volume.

However, the RHS of Fig. 1 might probably indicate the onset of a multifragmentation process. Therefore, the results in Fig. 1 indicate that compressional energy is more efficient than thermal energy in breaking nuclei. These results might also suggest that a liquid-gas phase transition, as proposed in (Minich, 1982) (see the lecture of D. Scott for an extensive discussion) could possibly not occur because the nucleus breaks during its expansion. Therefore, it would not be possible to get a low central density region where the compressibility is negative, a condition necessary for a gas-liquid phase transition to occur. The fact that, for the same amount of excitation, compression break nuclei more easily than thermal excitation can be understood by establishing an analogy with fission. In this latter case one can either heat a compound nucleus (thermal excitation) or give it some initial kinetic energy in the fission mode (collective energy). For the same amount of excitation, fission will occur more easily in the second than in the first case. We are here in a similar situation when comparing compressional with thermal energy.

b) Probing the temperature

In the preceeding subsection we have compared the efficiency of compressional and thermal energies for breaking nuclei. For that reasons we have started with equilibrium solutions for

the initial conditions. However, in heavy ion collisions one has very likely to consider more exotic species which are probably out of equilibrium as far as some of the macroscopic variables are concerned. For this reason it is also interesting to start with initial densities which are not the result of a self consistent calculation. For instance, starting from a static self consistent calculation of the ground state, one can assume a temperature different from zero while keeping the density profile fixed. However, in doing so it is important to note that changing the temperature of a nucleus while keeping its density profile fixed is a process which also changes the compressional energy.

The excited systems which are formed in heavy ion collisions have a temperature which changes during their dynamical evolution. Experimentally, one measures the temperatures by means of different probes (for instance by looking at light emitted particles). However, these probes allow to get the temperature only at a certain period of the life of the excited system. Therefore, probes testing the temperature at different instants of time can lead to different values of the temperature.

In order to illustrate what has been said above we have performed the following calculation : we have generated a density profile for the ^{208}Pb nucleus at T=0 MeV and for $\lambda = 0.2$ MeV/fm^{-2}. Then we have heated up the nucleus at T=35 MeV keeping the density profile unchanged during this operation. The subsequent evolution of the system is then followed by solving the TDTF equations. In Fig. 2 we show the density profile of the system at different steps of the evolution. As we can see, the system expands rapidly and at instants t=8, 16, 32 and 48 $\times$ 10^{-23}s the system has cooled to T=14, 9.4, 9 and 7.2 MeV respectively. Compared to the RHS of Fig. 1 the system breaks up in a smoother and more gradual way, probably because of the rapid expansion. If such an exotic behaviour would exists in heavy ion collisions, then the precise observation time becomes an all important parameter in the determination of the nuclear temperature. For instance, if a given probe becomes effective at t $\sim$ 2 $\times$ 10^{-22}s, say, then the observed temperature will be very different from its initial value because the system has already cooled down appreciably.

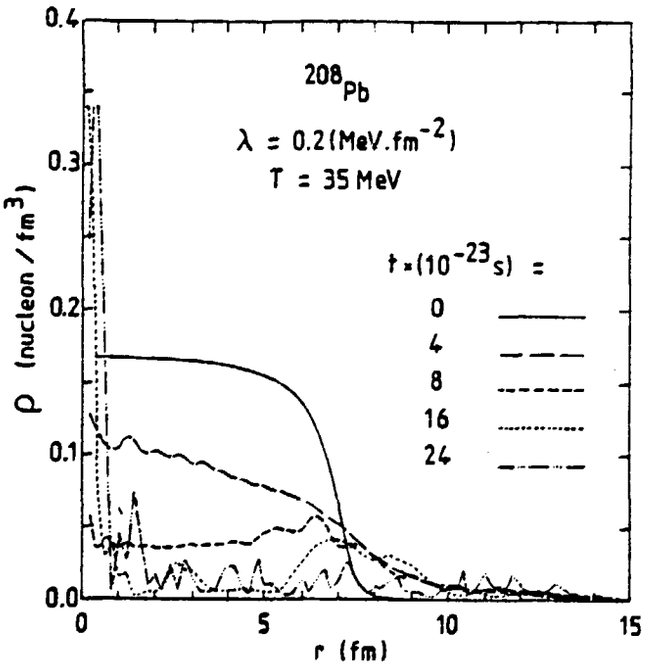

Fig. 2 Five sequential density profiles of ^{208}Pb, represented by 5 different graphs for instants t=0, 8, 16, 32 and 48 $\times$ 10^{-23}s, plotted against the nuclear radius, r, for $\lambda = 0.2$ MeV/fm^{-2} and an initial temperature for the ground state of T = 35 MeV.

c) Dissipation

Up to now the dynamical evolution of the system was not dissipative and the total entropy was conserved. If one mocks up two body collisions by a dissipative term, as proposed in section II, one can start with the ground state of ^{208}Pb and apply to it an initial velocity field

which pushes the density inwards. However, because of dissipation a large part of the energy in the collective flow will be transformed in excitation energy (heat). At th same time the entropy increases. In Fig. 3 we present an illustration of the influence of dissipation : the starting density was that of ^{208}Pb at T=0. The initial velocity field (proportional to r^2 has such a strenght that the collective energy has a magnitude of the order of the relative kinetic energy of 2 nuclei at ~ 20-50 MeV/u. At the beginning the system is compressed and its temperature increases due to both dissipation and compression. Then the temperature oscillates a bit at the beginning of the expansion because of two opposite effects : the expansion which tends to decrease T and dissipation which tends to increase T. As we can see in Fig. 3 the nucleus finally breaks up.

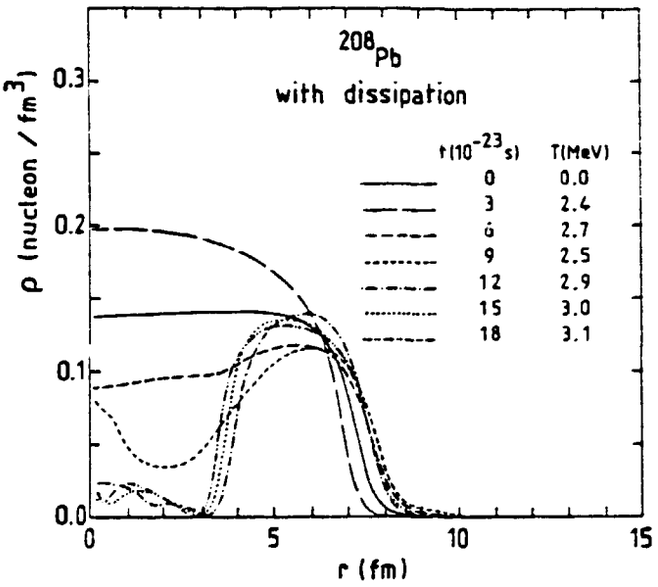

Fig. 3 Five sequential density profiles of ^{208}Pb, represented by 7 different graphs for instants T=6, 12, 18, 24, 30 and 36 × 10^{-23}s, plotted against the nuclear radius r. The initial conditions correspond to the ^{208}Pb nucleus at T=0 and an initial velocity field is applied. A dissipative term of the form discussed in section I has been included.

CONCLUSION

We have used a spherically symmetric TDTF approach to investigate the dynamical instabilit.es of hot and compressed nuclei over a time scale of the order of a few 10^{-22}s. We found that, for the same amount of energy, compression is more efficient than thermal excitation for breaking up nuclei. This is essentially due to the collective nature of the compressional energy. A possible implication of these results is that multifragmentation processes observed in heavy ion collisions could more likely be due to a mechanical instability than to a chemical instability.

REFERENCES

Quentin, P., and H. Flocard (1979). Ann. Rev. of Nucl. Part. Science, 28, 523.

Bonche, P., S. Koonin and J.W. Negele (1976). Phys. Rev. C13, 1226 ; Negele, J.W. (1982). Rev. Mod. Phys. 54, 913 and ref. therein.

Brack, M., C. Guet and H.B. Hakansson. Phys. Rep. in press and ref. therein.

Nemeth, J., M. Barranco, C. Ngô and E. Tomasi (1985). Z. Phys. A320, 691.

Dalili, D., J. Nemeth and C. Ngô. Z. Phys. in press.

Levit, S. (1984). Phys. Lett. 139B, 147 ; Suraud, E., and D. Vautherin (1984). Phys. Lett. 138B, 325.

Minich, R.W., S. Agarwal, A. Bujak, J. Chuang, J.E. Finn, L.J. Gutay, A.S. Hirsch, N.T. Porile, R.P. Scharenberg, B.C. Stringfellow and F. Turkot (1982). Phys. Lett. 118B, 458.